EUROPHYSICS LETTERS 1 October 2002

Europhys. Lett., **60** (1), pp. 72–78 (2002)

Energy dissipation and permeability in porous media

M. Pilotti[1], S. Succi[2] and G. Menduni[3]

[1] *Dipartimento di Ingegneria Civile, Università degli Studi di Brescia via Branze 38, 25123 Brescia, Italy*
[2] *Istituto per le Applicazioni del Calcolo M. Picone v.le del Policlinico 137, 00161 Roma, Italy*
[3] *DIIAR, Politecnico di Milano - P.zza Leonardo da Vinci 32, 20133 Milano, Italy*

(received 25 January 2002; accepted in final form 28 June 2002)

PACS. 47.55.Mh – Flows through porous media.
PACS. 47.15.Gf – Low-Reynolds-number (creeping) flows.
PACS. 47.85.Dh – Hydrodynamics, hydraulics, hydrostatics.

Abstract. – We investigate flow through porous media by solving the Navier-Stokes equations in 3D porous structures using the lattice Boltzmann method. We analyse the distribution of local specific dissipation of mechanical energy and we use this quantity to investigate the microscopic origin of absolute permeability. The averaging of this quantity on a flow cross-section provides a methodology to locate energy losses and to spot the appropriate scale of the permeability Representative Elementary Volume (REV). The effectiveness of the approach is shown by a numerical study of the flow field in simplified porous media for which experimental results are available.

Following up early works on lattice Gas Cellular Automata and lattice Boltzmann [1], which demonstrated the possibility of computing the absolute permeability of rock samples in 2D and in 3D, several papers over the last years have demonstrated the capabilities of LGA and LBM techniques to solve Navier-Stokes equations in complex geometries and to compute the mesoscopic properties of porous media (*e.g.*, *inter alia*, [2]). Accordingly, it is clear that these methods can theoretically be used to complement laboratory tests, providing insights into the flow dynamics in complex structures that should make it possible to explore the origins of dissipative processes and of upscaling of rock properties (*e.g.*, [3]). In this direction, some papers have recently explored the distribution of either computed flow velocity (*e.g.*, [4]) inside simple reconstructed porous media or of kinetic energy (*e.g.*, [5]) in 2D flow fields. This research direction is of utmost importance, since it will help explaining, from a theoretical point of view, the origin of absolute permeability K. However, absolute permeability is an average quantity that should be measured on a representative elementary scale and is closely related to energy dissipation on a smaller scale. In this direction we argue that kinetic energy and velocity distributions provide a useful but not conclusive answer to this problem.

Restricting our attention to the incompressible, isothermal and stationary flow of a Newtonian fluid, in this contribution we suggest analysing the distribution in a flow field

of the local rate of dissipation of mechanical energy per unit mass of fluid due to viscosity, given by

$$\phi = \frac{2\mu}{\rho} e_{ij} e_{ij}, \tag{1}$$

where μ [Pa s^{-1}] is the first dynamic viscosity coefficient and ρ [kg m^{-3}] the fluid density. Here $e_{ij}(x, y, z)$ is a symmetrical strain tensor defined as

$$e_{ij} = \frac{1}{2}\left(\frac{\partial u_j}{\partial x_i} + \frac{\partial u_i}{\partial x_j}\right), \tag{2}$$

$\boldsymbol{u}(x, y, z)$ being the velocity of the fluid at position (x, y, z). Since quantity (1) is closely related to the local energy dissipation per unit mass of fluid, it can be related to the dissipative processes which act on a larger scale, as originally shown by Prager and Weissberg [6], who theoretically derived a variational upper bound on the permeability by minimizing the overall rate of energy dissipation for the creeping flow within the intergranular space between penetrable spheres. In particular, quantity (1) governs the evolution of the total head $H(x, y, z)$,

$$H(\boldsymbol{x}) = \frac{p}{\rho} + \frac{u^2}{2}, \tag{3}$$

i.e. the specific energy per unit mass of fluid at position $\boldsymbol{x}, p$ being the local pressure. If a suitable average is taken of this quantity over the flow field, its drop can be interpreted in terms of an overall friction coefficient which, in the case of saturated flow in porous media, is closely related to the absolute permeability. To demonstrate this point, let us consider, for example, the flow field in an isotropic porous medium across which an assigned pressure drop is applied. Here an effective flow direction can be identified and a cross-section A [m^2] can be defined as the 2D subspace orthogonal to this direction. Let s be the curvilinear coordinate along the average flow direction and Q [m^{3}s^{-1}] the volumetric discharge through the cross-section, then

$$\underline{H}(s) = \underline{H}(0) - \frac{1}{\rho Q}\int_0^s \int_{A(s)} 2\mu e_{ij} e_{ij}\, \mathrm{d}A\, \mathrm{d}s \tag{4}$$

provides the variation of the average total head $\underline{H}(s)$ at cross-section $A(s)$, a quantity that is introduced when a one-dimensional approach is adopted. Since the same quantity $\underline{H}$ appears in the empirical Darcy's law valid at the REV scale, the scalar absolute permeability coefficient can be computed as a function of s, as

$$k(s) = \frac{\mu Q^2 s}{A} \cdot \frac{1}{\int_0^s \int_{A(s)} 2\mu e_{ij} e_{ij}\, \mathrm{d}A\, \mathrm{d}s}. \tag{5}$$

Accordingly, the local rate of dissipation (1) provides a continuous quantity (5) whose mesoscopic counterpart, K, is of great interest for the study of flow in porous media. Usually, in most applications the absolute permeability K is computed using the overall head drop across a plug and the corresponding effective velocity, Q/A. It might be important to emphasize that both approaches can be used to compute K. However, whilst the latter assumes the knowledge of the minimum linear scale of the representative elementary volume scale for permeability, say S, a quantity that is *a priori* unknown, relations (4) and (5) provide the overall energy dissipation as a continuous function of s (see figs. 2 and 4b below), allowing a straightforward evaluation of S on the basis of the analysis of the $k(s)$ function. Whilst the identification of the REV

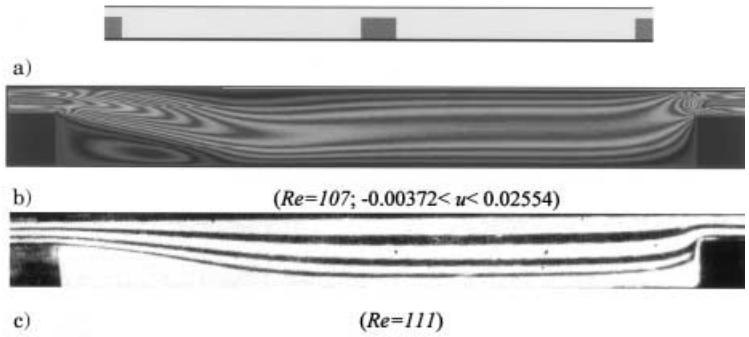

Fig. 1 – Longitudinal section of a labyrinth seal (a), as numerically investigated in this work. Here $\Delta/\delta = 1.49$, where Δ is the gap width and δ is the step height and 2δ the step length. In (b) a map of the longitudinal velocity component u [l.u./t.u.] is shown through an elementary cell of the seal. All units are lattice units. (c) is a photograph taken during the prototipal experiment [9]. Flow enters the seal from the left.

scale can be performed also by increasing the computational domain size in a step-wise fashion and computing the overall head drop across the plug until convergence to a well-defined limit is verified (*e.g.*, [7]), $\underline{H}(s)$ and $k(s)$ are by definition continuous functions that provide clear indications on the variation of total average head and overall dissipation on each cross-section in the direction of the effective flow. Since $k(s)$ is obtained by integration of the local rate of dissipation of mechanical energy (1), the boundary features that determine $k(s)$ can be easily located by inspecting the space distribution of (1), something that could not be done by computing K in the usual way, *i.e.* by using averaged quantities on the cross-section that hide local details and do not allow this type of analysis. An example will be briefly shown in the following.

Over the last few years several experiments have been published in the literature using reconstructed porous media [8] and comparing numerical estimates of permeability with experimental results. However, since the numerical specimens are inevitably smaller than the laboratory ones due to computational constraints, it has not been clarified what the least linear space scale S is at which absolute permeability can be computed. To this purpose we believe that although permeability is, dimensionally, a geometric quantity, its determination on the basis of geometry would yield only a partial picture of the problem. Rather, it must be evaluated on the basis of its energetic implications, that are clearly revealed by (5) as a function of s. We believe that the determination of this point would shed light on the possibility of devising numerical experiments for testing upscaling mechanisms and would provide information on the minimum numerical effort needed to numerically reproduce the permeability of larger prototypal specimens.

In the following we apply the proposed approach to the slow viscous flow inside a labyrinth seal and through a regular spherical-bead packing. As far as the first application is concerned, it has been chosen for the availability of detailed experimental measurements [9], which can be used to test the reliability of the numerical solution in a high-relative roughness geometry that provides a simplified picture of the flow field inside a porous medium. In particular, the flow field inside a rectangular duct with gap height Δ has been investigated, where a regular sequence of rectangular obstructions of height δ and length 2δ is present (see fig. 1a). In the numerical experiments the pressure and velocity fields have been computed by using a $d3q19$ LBM solver [10] that has been implemented to this purpose. No-slip conditions along solid boundary and periodic conditions between the inlet and the outlet have been imposed

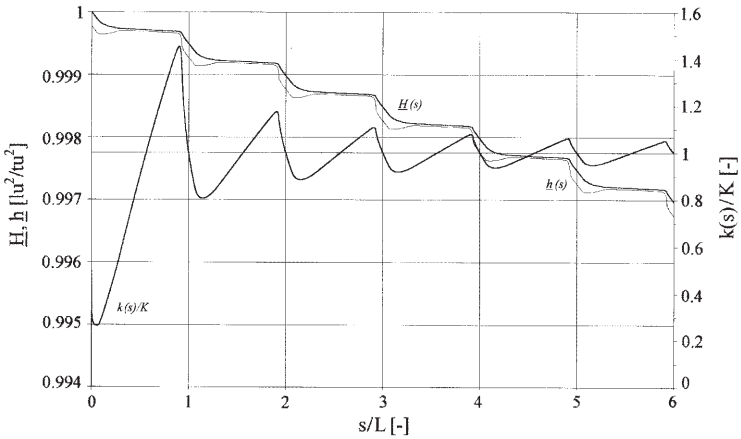

Fig. 2 – The total $\underline{H}$ (thick line) and piezometric $\underline{h}$ (thin line) head with the $k(s)/K$ pattern along a regular sequence of elementary cells of the seal. Please note the pressure rise and head loss behind each abrupt expansion, a well-known effect in hydraulics, named after Borda ($\Delta/\delta = 1.49$, $Re = 107$). By subtraction of the two heads, the average kinetic energy per unit mass on each cross-section s can be obtained. The $k(s)/K$ pattern along the seal allows to identify the minimum linear scale for K.

on an elementary cell of the periodic array in the prototypal seal. We have explored the relative roughness range $\Delta/\delta = 1.2$ and 1.49, with Reynolds number ($Re = 2Q/(\nu b)$, where $b = 1$ is the duct width and ν is the fluid kinematic viscosity) varying between 1 and 400 for $\Delta/\delta = 1.49$. There is a close resemblance between the photographed and the numerically computed flow fields in the same Re range, both as far as the streamlines pattern and the presence and extension of recirculation cells are concerned. When $Re > 5$, a recirculating region is observable immediately downstream of the step. When Re grows higher (*e.g.*, in the case portrayed in figs. 1b and c) a second smaller vortex develops immediately upstream of the step. Eventually, for the highest simulated Re, intermediate smaller and weaker eddies can be detected. For the labyrinth seal of fig. 1, in place of permeability it is more usual in applied fluid mechanics to compute a friction factor λ [-] ([-] stands for non-dimensional quantity), typically defined through the Darcy-Weisbach relation

$$\lambda = -\frac{8RA^2}{Q^2}\frac{\Delta \underline{H}}{L}, \tag{6}$$

where R [m] is the boundary related hydraulic radius. In the field of validity of Darcy's law it is easy to show that the relationship

$$\lambda = \frac{f}{Re} \tag{7}$$

holds, where f [-] is a constant that depends on boundary geometry only. Accordingly, it is possible to write

$$K = \frac{32R^2}{f}, \tag{8}$$

and the hyperbolic pattern (7) is equivalent to a constant permeability K as given by Darcy's law. Our numerical results are in extremely good agreement with the measured friction factor λ (error $< 3\%$), even for the highest values of Re explored in the experiments, where a

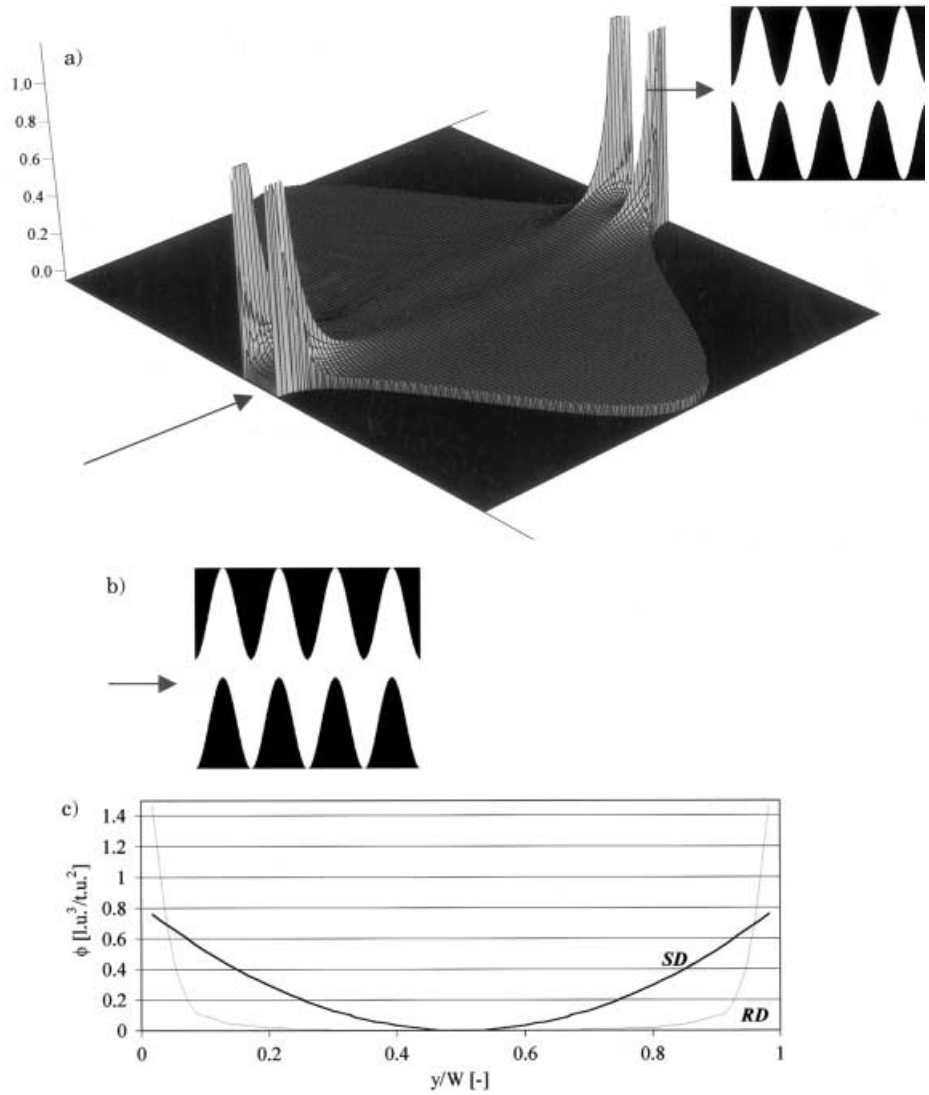

Fig. 3 – Map (a) of local adimensional dissipation $\phi/\phi_{\max}$ along an elementary cell of a duct characterized by the boundary with the regular roughness shown at the upper right corner, when $Re = 1.49$. Flow enters the duct from the left, as shown by the arrow. In (b) the same porous medium where the lower boundary has been shifted of 1/2 wavelength to the right. (c) compares the local dissipation distribution in the throat of case (a) (rough duct, RD) with the one in the cross-section of a rectangular smooth duct (SD) having the same width W, when the discharge is equal in the two cases. Note the significant sharpening of the dissipation profile near the solid wall, showing that most of the contribution to overall dissipation is confined to a small region of the sample.

significant departure from Darcy's law can be observed, a well-known effect due to the growing importance of the convective term in the Navier-Stokes equation.

In addition to the overall permeability K across the elementary cell, in this paper we emphasize the importance of the variation of $\underline{H}(s)$, as given by (4). This is portrayed in fig. 2,

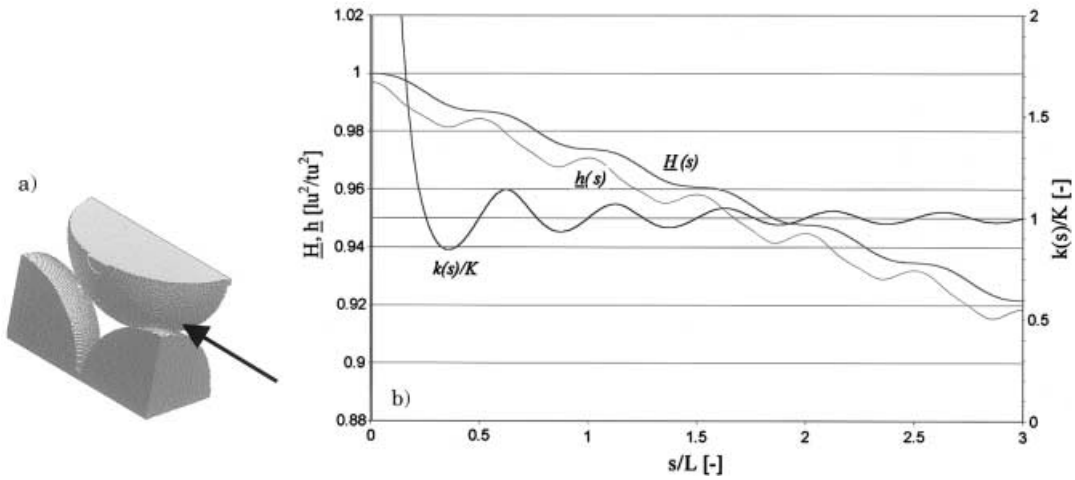

Fig. 4 – Elementary cell (a) for the simulation of creeping flow through a face-centered-cubic spherical-bead packing of maximum concentration. The fluid flows from the right to the left, in the direction of the arrow. In (b) the total $\underline{H}$ (thick line), piezometric $\underline{h}$ (thin line) head and the $k(s)/K$ pattern are shown along a porous medium made up of a sequence of elementary cells of the cubic packing. Here the average kinetic energy per unit mass has been magnified to enhance the separation between the two lines. Again, note the pressure rise behind the gradual intergranular space expansions ($Re = 0.07$).

where $\underline{H}(s)$ and $\underline{h}(s)$ (the pressure-related term, obtained by subtracting the averaged kinetic energy contribution to $\underline{H}$) are shown along a regular sequence of elementary cells. This type of representation, which is akin to that used in pipe flow analysis, allows the identification of the REV scale and provides a clear indication of the relative importance of single dissipative processes inside the flow field. It is here possible to observe both the distributed energy grade along the conduit and the energy loss due to the abrupt expansion and contraction behind and in front of the step. In particular, the abrupt expansion causes an energy loss which can be easily evaluated by extrapolating the head line $\underline{H}(s)$ in fig. 2 and which, in itself, is greater than the overall energy loss along the gap. The ratio between the localized energy loss at the sudden gap contraction and the head loss at the expansion is approximately 0.4. The $k(s)/K$ pattern clearly shows that, while the minimum scale S at which permeability could be exactly computed is the full length L of an elementary periodic cell, if one randomly selects a stretch l of duct, in order to keep the error on the computed permeability within a 10% error it must be at least $l/L > 4$. In addition, fig. 2 easily allows to locate the major geometric sources of overall dissipation. These can be further inspected by considering the $\phi(x, y, z)$ map, that provides guidances to a possible boundary redesign. We will show this possibility with reference to another high-relative-roughness duct, shown in fig. 3a. Figure 3a shows the longitudinal map of local dissipation (1) inside the elementary cell of the duct partly shown in the upper right corner, when $Re = 1.49$, being here the linear dimension provided by the volumetric height. As can be seen, the largest contribution to the overall energy loss arises in correspondence to the maximum duct contraction. In order to avoid it, if we shift the lower boundary 1/2 wavelength ahead (see fig. 3b), we neither change the hydraulic radius nor the porosity; however our numerical simulations show that there is a 87% increase of the permeability!

For the sake of simplicity, we have so far investigated high-relative-roughness plane flow

fields, but the same methodology can be applied to three-dimensional flow fields, such as the one through a face-centered-cubic spherical-bead packing of maximum concentration (porosity $\phi = 0.2595$ [-]) investigated in [4]. Here we have taken full advantage of the symmetry of this packing and we have considered the elementary cell shown in fig. 4a. Along the side walls of the specimen, periodicity boundary conditions have been imposed, whilst along the solid boundary a first-order–accuracy non-slip condition has been imposed. By operating with a $68 \times 95 \times 134$ discretization of the boundary, our computed permeability is within 1% of that computed in [4]. In fig. 4b we show the variation of $\underline{H}(s)$, $\underline{h}(s)$ and $k(s)/K$ along the reconstructed specimen, when $Re = UD/\nu = 0.07$ (here D is the grain diameter and U is the average flow velocity over a cross-section). From these patterns it is easy to spot the minimum linear dimension needed to keep the error on the permeability below an assigned threshold.

In conclusion, the use of relationship (5) provides a way to identify the minimum linear scale for the evaluation of the permeability REV, and the space distribution of the rate of dissipation of mechanical energy (1) highlights the boundary sources of energy dissipation that determine, on a larger scale, the local absolute permeability.

REFERENCES

[1] Rothman D. H., *Geophysics*, **53** (1988) 509; Cancelliere A., Chang C., Foti E., Rothman D. H. and Succi S., *Phys. Fluids A*, **2** (1990) 2085.
[2] Olson J. F. and Rothman D. H., *J. Fluid Mech.*, **341** (1997) 343; Lowe C. and Frenkel D., *Phys. Rev. Lett.*, **77** (1996) 4552.
[3] Sahimi M., *Rev. Mod. Phys.*, **65** (1993) 1393; Martys N. S., Torquato S. and Bentz D. P., *Phys. Rev. E*, **50** (1994) 403.
[4] Maier R. S., Kroll D. M., Kutsovsky Y. E., Davis H. T. and Bernard R. S., *Phys. Fluids*, **10** (1998) 60.
[5] Andrade J. S. jr., Almeida M. P., Mendes Filho J., Havlin S., Suki B. and Stanley H. E., *Phys. Rev. Lett.*, **79** (1997) 3901.
[6] Prager S., *Phys. Fluids*, **4** (1961) 1477; Weissberg H., *J. Appl. Phys.*, **34** (1963) 2636.
[7] Pan C., Hilpert M. and Miller C. T., *Phys. Rev. E*, **64** (2001); Van Genabeek O. and Rothman D. H., *Ann. Rev. Earth Sciences*, **24** (1996) 63.
[8] Adler P. M., *Porous Media* (Butterworth-Heinemann, London) 1992; Pilotti M., *Transport Porous Media*, **33** (1998) 257; **41** (2000) 359.
[9] Lazzari F., *Energia Elettr.*, **7-8** (1975) 353.
[10] Succi S., Benzi R. and Higuera F., *Physica D*, **47** (1991) 219; Benzi R., Succi S. and Vergassola M., *Phys. Rep.*, **222** (1992) 3; Pilotti M. and Menduni G., *Earth Surf. Proc. Landforms*, **22** (1997) 885; Higuera F., Succi S. and Benzi R., *Europhys. Lett.*, **9** (1989) 345.